2. Revision

A fast open data reduction workflow for the electron microprobe flank method to determine $Fe^{3+}/\Sigma Fe$ contents in minerals

Dominik C. Hezel[1], Heidi E. Höfer[1], Andreas Fichtner[2]

[1]Goethe-Universität Frankfurt, Altenhöferallee 1, 60438 Frankfurt am Main, Germany
dominik.hezel@em.uni-frankfurt.de
[2]ETH Zürich, Institut für Geophysik, Sonneggstrasse 5, 8092 Zürich, Schweiz

**corresponding author:* Dominik Hezel- dominik.hezel@em.uni-frankfurt.de

keywords: flank method, garnet, ferrous/ferric iron, data reduction, python

2. revision to *American Mineralogist*

November, 2023

Formatting:	Times New Roman, 12 pt, double spacing
Pages (main text):	13
Words (main text):	4019
Words (abstract):	204
Figures:	7
Tables:	0
Spelling:	British English

Abstract

Knowing the $Fe^{3+}/\Sigma Fe$ ratio in minerals is important to understand the formation and evolution of minerals and their host rocks. Variable $Fe^{3+}/\Sigma Fe$ in *e.g.*, garnet is accompanied by a change of their characteristic FeLα and FeLβ X-ray emission lines, which can be quantified with electron microprobe measurements using the flank method. The required data reduction process to determine the $Fe^{3+}/\Sigma Fe$ remained complex. Here we present a new data reduction tool taking garnet data as an example. This new *Flank Reduction* app is a freely-available, graphical user interface-driven, web-based application to reduce flank method data quickly and easily. The entire data reduction process is achieved in minutes compared to hours or days, as it was before. Flank Reduction provides comprehensive insights into *e.g.*, the employed flank method standards, obtained data, or errors, through a wide array of controls and visualisation tools. Documentation with comprehensive information on the flank method, data reduction, as well as training material such as video tutorials or sample datasets are available on a dedicated webpage. Flank Reduction emphasises the high value of FAIR (Findable, Accessible, Interoperable, Reproducible) and open research software and demonstrates how current developments in coding and app implementation can facilitate the development of powerful and expandable research software.

1. Introduction

The iron oxidation state in minerals such as metamorphic garnet, pyroxenes or amphiboles provides important information on the redox state of these minerals and their host rocks at the time of last equilibration. The ambient oxygen fugacity prevailing in a rock when a mineral equilibrates with its surroundings is recorded in its $Fe^{3+}/\Sigma Fe$ ratio (throughout this work this ratio refers to a wt%-ratio). The *in-situ* determination of $Fe^{3+}/\Sigma Fe$ on a µm-scale in a mineral by electronprobe microanalysis (EPMA) is possible with the flank method (Höfer and Brey 2007). This method has been developed over the past decades in a series of papers by Höfer et al. (1994), Höfer et al. (1996), Höfer et al. (2000), Höfer (2002), and brought to its final state in Höfer and Brey (2007). The flank method has been applied to garnets (*e.g.*, Wang et al. 2022; Tang et al. 2019, Gudelius et al. 2019, Tao et al. 2018, Malaspina et al. 2009, 2010), sodic amphiboles (Enders et al. 2000), wuestite (Höfer et al. 2000; Longo et al. 2011), and glasses (Zhang 2018). It can potentially be applied to other minerals of interest, such as pyroxenes (Höfer et al. 2004).

In brief, the flank method works as follows: The wavelengths and intensities of the characteristic FeLα and FeLβ X-ray emission lines of a mineral such as garnet depend on its $Fe^{3+}/\Sigma Fe$ as well as its ΣFe. Figure 1 shows this dependency exemplified in spectra of an Fe^{2+}-bearing garnet (almandine) and an Fe^{3+}-bearing garnet (andradite). The *x*-axis of Figure 1 represents the analyser crystal position of a JEOL EPMA spectrometer. The $Fe^{3+}/\Sigma Fe$ of a mineral such as garnet is quantified by the count-rates obtained at two fixed analyser crystal positions: one at the flank of the FeLα line, and one at the flank of the FeLβ line (vertical dashed lines in Fig. 1). As the spectrum of a garnet changes with changing $Fe^{3+}/\Sigma Fe$ and ΣFe, so do the count-rates at these fixed analyser crystal positions. Hence, the count-rates at these flanks of garnets correlate with their $Fe^{3+}/\Sigma Fe$ and ΣFe. The sensitivity of this correlation is at

its maximum, where the change of the count-rate is maximal. This is where the difference between the count-rate of an Fe^{3+}-poor and Fe^{3+}-rich garnet is maximal (dashed lines in Fig. 1). Out of convention, we are not using the difference in count-rates between the FeLα and FeLβ flank measurements, but their ratio FeLβ/FeLα, which is subsequently abbreviated as Lβ/Lα.

The measured FeLβ/FeLα ratios and Fe concentrations (=ΣFe) of several flank method garnet standards with their known Fe^{3+}/ΣFe are used to calculate a 2D linear regression (from now on called 'regression'). This regression provides a set of parameters to (i) calculate the Fe^{3+}/ΣFe in minerals with unknown Fe^{3+}/ΣFe, as well as (ii) lines of equal Fe^{3+}/ΣFe in a plot of ΣFe vs. Lβ/Lα (Fig. 2) to visualise the measured data.

The flank method is particularly suitable when mineral grains are zoned or too small for other methods such as Mössbauer spectroscopy, or XANES, both with with insufficient spatial resolution, or when these methods are unavailable. An advantage of the flank method is the simultaneous Fe^{3+}/ΣFe and quantitative elemental analysis at each measured spot.

Applying the flank method requires two workflows:

(i) *Determining analyser crystal positions*: Höfer and Brey (2007) use the FeKα 9th order line to determine the analyser crystal positions to measure the Fe L-line flanks, as this line sits in between the FeLα and FeLβ lines. This required specialised software to determine the peak of the FeKα 9th order line, as well as a dedicated Excel spreadsheet.

(ii) *Data reduction to determine Fe^{3+}/ΣFe*: Höfer and Brey (2007) describe two options for data reduction, one quicker, but less precise, and a second – the regression mentioned above – which is a more complex and precise procedure.

Both options require a complex combination of numerous Excel spreadsheets, and, for the regression, the conversion of selected spreadsheets to text files which are then fed to and processed with the Matlab clone Octave. This workflow required a trained expert and can quickly take up to several days. Re-running it – *e.g.*, to test variations of certain

parameters or standards – is almost equally time-consuming. Finally, the procedure requires proprietary software and is not openly accessible.

Both workflows remained largely unchanged over the years, even though additions have been made to the spreadsheets. These patches made the entire process increasingly complex. Hence, the data reduction process could not be performed without extensive hands-on training, although the measurement itself could be reproduced fairly straightforwardly.

Here we present an entirely new data reduction tool we call *Flank Reduction* that uses the precise regression method (eq. 2 in Höfer and Brey 2007). The entire data reduction is processed within a simple-to-use web-application that has a graphical user interface (GUI) as well as many new and additional functionalities. The entire data reduction workflow now takes only minutes and can be re-run with changed parameters, as often as necessary within seconds. We further reimagined a simple procedure for the positioning of the analyser crystals, for which the web-application provides a dedicated helper tool. Finally, we embedded the web-application in a data reduction platform.

2. Methods

Coding

The code for the new data reduction procedure and analyser crystal positioning tool is written in Python. The GUI of the web application, including all interactive elements, styling, *etc*. is implemented using the Streamlit (streamlit.io) programming framework and published through the Streamlit community cloud. All diagrams are realised with the Bokeh and Plotly libraries *i.e.*, all plots can be interactively controlled, downloaded as image files, and informative features such as tooltips (context information when hovering over a data point) have been added. The entire code, requirements, data files, *etc*. are hosted and published under

the MIT License, *i.e.*, openly accessible GU Frankfurt, Institut für Geowissenschaften GitHub repository (GeoSci-FFM/flank-method). Finally, the Quarto web-publishing framework is used to provide in-depth flank method background information, code and workflow documentation, training material, video tutorials (hosted on YouTube), test datasets, a flank method section for publications, literature, and more information surrounding the flank method and the entire data reduction web-application. Everything can be accessed through the free and open geoplatform.de website. We follow and support with this approach the call for FAIR (Findable, Accessible, Interoperable, Reproducible) open-source publication (*e.g.*, Lehnert et al. 2021; Klöcking et al. 2023; Wilkinson et al. 2016 and references therein), and more specifically for FAIR4RS (for Research Software; Barker et al. 2022) publication.

Measurement program, standards & parametrisation

In the quantitative analysis measurement program, the Fe L-lines are measured on the flanks of the FeLα and FeLβ peaks as described above, and the Fe-concentration is measured by EMPA, using conventional methods.. At least all major elements need to be measured for an accurate matrix correction, and optional elements of interest – such as trace elements – may be added. Each sample is measured with a grid of *e.g.*, 5x5 (*i.e.*, total of 25) spot analyses. Details and examples on how to set-up the measurement program, naming conventions for the samples and flank method standards (*i.e.*, standards with known Fe-concentration and $Fe^{3+}/\Sigma Fe$ ratio), structure, and requirements of the sample file, *etc*. can be found on the flank method website.

It is required to measure at least four flank method standards at the beginning and end of a measurement campaign. For a better precision, we recommend using more than the required four flank method standards, and ideally with a substantial spread in Fe^{3+} and ΣFe that covers the expected range in Fe^{3+} and ΣFe of the samples. The used flank method standard data

need to be part of the Flank Reduction standard file that is stored alongside the program on GitHub. Alternatively, a self-produced file with additional standard compositions can be uploaded. The standard file, its entries and structure are detailed on the Flank Reduction website.

Mathematically, the flank method rests on the assumption that the Fe^{3+} concentration can be modelled as

$$Fe^{3+} = -A - B\frac{L\beta}{L\alpha} + (1 - C)\Sigma Fe + D\frac{L\beta}{L\alpha}\Sigma Fe \quad (Eq.\ 1),$$

which is identical to Eq. 2 in Höfer and Brey (2007), but rearranged to have Fe^{3+} on the left-hand side. In the interest of a more condensed notation we rewrite Eq. 1 as

$$z = a + bx + cy + dxy \quad (Eq.\ 2),$$

where we define $z = Fe^{3+}$, $a = -A$, $b = -B$, $c = 1 - C$, $d = D$, $x = \frac{L\beta}{L\alpha}$ and $y = \Sigma Fe$. To estimate the four coefficients a, b, c, and d (or, equivalently A, B, C, and D), we rely on $N \geq 4$ measurements of x, y, and z from flank method standards, which we denote by x_i, y_i, z_i, respectively. The subscript $i = 1, \ldots, N$ is the running index of the standard samples. Due to measurement errors and unmodelled effects in Eq. 1, it is neither possible nor desirable to find coefficients a, b, c, and d such that the observations z_i are explained exactly. Instead, we try to minimise the least-squares misfit

$$\chi = \frac{1}{2}\sum_{i=1}^{N}\frac{1}{\sigma_i^2}(a + bx_i + cy_i + dx_iy_i - z_i)^2 \quad (Eq.\ 3),$$

where the σ_i denote the standard deviations of the measurement errors in Fe^{3+} of the individual standards (*i.e.*, the standard deviation of z_i). Forcing the partial derivatives of Eq. 3 with respect to the coefficients a, b, c, and d to 0 leads to a system of four linear equations,

$$\sum_{i=1}^{N}\frac{z_i}{\sigma_i^2} = a\sum_{i=1}^{N}\frac{1}{\sigma_i^2} + b\sum_{i=1}^{N}\frac{x_i}{\sigma_i^2} + c\sum_{i=1}^{N}\frac{y_i}{\sigma_i^2} + d\sum_{i=1}^{N}\frac{x_iy_i}{\sigma_i^2} \quad \text{(Eq. 4.1)},$$

$$\sum_{i=1}^{N}\frac{x_iz_i}{\sigma_i^2} = a\sum_{i=1}^{N}\frac{x_i}{\sigma_i^2} + b\sum_{i=1}^{N}\frac{x_i^2}{\sigma_i^2} + c\sum_{i=1}^{N}\frac{x_iy_i}{\sigma_i^2} + d\sum_{i=1}^{N}\frac{x_i^2y_i}{\sigma_i^2} \quad \text{(Eq. 4.2)},$$

$$\sum_{i=1}^{N}\frac{y_iz_i}{\sigma_i^2} = a\sum_{i=1}^{N}\frac{y_i}{\sigma_i^2} + b\sum_{i=1}^{N}\frac{x_iy_i}{\sigma_i^2} + c\sum_{i=1}^{N}\frac{y_i^2}{\sigma_i^2} + d\sum_{i=1}^{N}\frac{x_iy_i^2}{\sigma_i^2} \quad \text{(Eq. 4.3)},$$

$$\sum_{i=1}^{N} \frac{x_i y_i z_i}{\sigma_i^2} = a \sum_{i=1}^{N} \frac{x_i y_i}{\sigma_i^2} + b \sum_{i=1}^{N} \frac{x_i^2 y_i}{\sigma_i^2} + c \sum_{i=1}^{N} \frac{x_i y_i^2}{\sigma_i^2} + d \sum_{i=1}^{N} \frac{x_i^2 y_i^2}{\sigma_i^2} \text{ (Eq. 4.4).}$$

The sums in Eqs. 4.1 - 4.4 are the knowns of the linear system and can be computed directly from the flank method standard measurements and their errors. Provided that the standard measurements are independent, the linear system of equations can be solved for *a*, *b*, *c*, and *d*. This is implemented using standard functions for linear system solutions with widely used Python packages.

A solution for *a*, *b*, *c*, and *d* is acceptable, when the differences between modelled and measured Fe^{3+} concentrations ($a + bx_i + cy_i + dx_iy_i - z_i$) are on average similar to the measurement standard deviations (σ_i), *i.e.*, when according to eq. 3 we have $\chi \approx \frac{N}{2}$. For $\chi \gg \frac{N}{2}$, the error standard deviations are either under-estimated or additional effects need to be considered. Conversely, $\chi \ll \frac{N}{2}$ typically signals that measurement errors have been over-estimated.

The $Fe^{3+}/\Sigma Fe$ ratio of the used flank method standards have been determined using Mössbauer spectroscopy and have similar standard deviations of about ±0.01 (1σ). We therefore simplify the four eq. 4.1 to 4.4. by assuming that the standard deviations of all standard samples are identical. The standard deviations – *i.e.*, all σ^2_i – can then be removed from eq. 4.1 to 4.4. For the same reason, we are not calculating χ to test whether the determined Fe^{3+} values are plausible. Instead, we determine the $Fe^{3+}/\Sigma Fe$ ratios of at least four flank method standards and compare these to the reported $Fe^{3+}/\Sigma Fe$ ratios determined by Mössbauer spectroscopy. In Höfer et al. (2017), it has been shown that the uncertainties in $Fe^{3+}/\Sigma Fe$ determination are similar for both methods.

3. Results

Figure 3 shows the schematic workflow of the flank method. Steps 2 and 3 remain largely unchanged to how flank method data have been reduced before, except for a few adjustments, of which the most important are explained below. Step 1 and in particular the entire step 4 of the data reduction process are new and described in the following two sections.

Determining the analyser crystal positions on the flanks of FeLα and FeLβ

Analyser crystal positions need to be determined at the beginning of a measurement campaign. Figure 1 shows FeLα and FeLβ spectra from an almandine (Fe^{2+}-rich) and an andradite (Fe^{3+}-ich) together with their difference spectrum. The collection of such spectra are time-consuming and unnecessary, and it is sufficient to measure small intervals across the minima and maxima positions of the difference spectrum (Fig. 4), which then usually takes less than 10 min. Such ’interval spectra‘ can be uploaded to a helper tool in Flank Reduction to identify the analyser crystal positions. The requirements for the file structure of the interval spectra are documented on the Flank Reduction website.

The analyser crystals need to be set at the minima and maxima of the difference spectrum (vertical, dashed lines in Fig. 1) to achieve a maximum dispersion of the lines of equal $Fe^{3+}/\Sigma Fe$ on the Fe^{3+} Results Plot (Fig. 2). A large dispersion directly translates to a better resolution and accuracy of the determined $Fe^{3+}/\Sigma Fe$. Therefore, the Lβ/Lα of a standard with high Fe^{2+} and ΣFe (*e.g.*, almandine) is useful as a quality check for the chosen positions as well as a long-term monitor for Lβ/Lα.

The flank data reduction procedure

The following describes the general workflow for the Flank Reduction program to illustrate how it works and highlights its core aspects such as ease of use, versatility, data

inspection capabilities, expandability, and speed. Further documentations are detailed on the Flank Reduction website.

Flank Reduction requires comma-separated value (csv) files in the UTF-8 format, which is an export format in almost all spreadsheet or similar programs. The spreadsheet with the measurements requires columns with the sample name, measured FeO-concentrations, and the flank FeLα and FeLβ intensities, as well as a copy of the sample name column, which is renamed to 'Inspected'. The benefit of this additional column is explained towards the end of section 3. Any additional measured element concentration column will be part of the results output file, while any other additional column is ignored. This spreadsheet is uploaded *via* the 'upload' button on the 'Data Upload & Reduction' page of Flank Reduction (Fig. 5) and can be displayed by expanding the box below the upload button. All tables of Flank Reduction are interactive, *e.g.*, sortable by clicking on a header, or searchable by using the cmd+F or ctrl+F keyboard shortcuts. Information on how to use each sub-page are provided in info-boxes on the sidebar of each sub-page.

If not selected otherwise, the first four standards from the uploaded spreadsheet are automatically selected and used to calculate the regression parameters according to eq. 1. As stated above, 25 spots are typically measured on a standard or sample. The averages of these 25 analyses of each sample are automatically calculated, and the $Fe^{3+}/\Sigma Fe$ ratios are calculated using the regression parameters. Similarly, the averages of the 25 analyses for all other elements in each sample are calculated. The results are immediately ready as a downloadable csv output file on the 'Output' page on the app webpage. This data reduction is done within seconds, compared to hours with the previous Excel sheets.

Visualisation and inspection of the results

The individual analyses of the uploaded data should be checked for outliers or other anomalies before calculating the results as described above. The 'Data Inspect' section is dedicated to inspecting the measurement results – drift during the measurements, the result from the regression – the results from the $Fe^{3+}/\Sigma Fe$ calculation, as well as to perform several quality checks. The Fe^{3+} Results Plot as shown in Figure 2 serves as the first quality check for the regression and Fe^{3+} determination. It immediately shows whether the standards chosen for the regression are suitable for the unknown samples. The plot should principally look as displayed, and with an ideally large dispersion of the lines of equal $Fe^{3+}/\Sigma Fe$. The flank method standards used for the regression can be selected and the selection instantly varied to identify the optimal regression. This means, the regression and dispersion of the lines of equal $Fe^{3+}/\Sigma Fe$ in the Fe^{3+} Results Plot depend on the selected set of flank method standards. Hence, this procedure is used to select the set of flank method standards that best represent the $Fe^{3+}/\Sigma Fe$ of the chosen flank method standards. To illustrate how an additional flank method standard changes the regression, Figure 2b shows the extreme and unreasonable case – given the set of Fe^{3+}-poor samples in this example – with an additional andradite standard. This changes the positions of the lines of equal $Fe^{3+}/\Sigma Fe$ in the region of the samples by about 0.02. The comparison of Figure 2a and b illustrates the importance of using standards with similar $Fe^{3+}/\Sigma Fe$ and ΣFe as the samples to produce accurate results.

The calculated $Fe^{3+}/\Sigma Fe$ can be displayed against various parameters such as element concentration or beam current to check whether these changes depend on the selected parameter, or the selected standards. This provides profound insights into the measurements, calculated results, or the suitability of the used flank method standards.

As mentioned, each sample is often analysed with a grid of a total of 25 points. Flank Reduction automatically calculates the average of this number of points, independent from how many analyses per sample have been acquired. To reduce the measuring time, the optimum

number of analyses can be found by testing how many analyses per sample are sufficient to still obtain an acceptable uncertainty of the results. To do this, only few samples – maybe 10 or 20 – are measured with 25 or even more analyses per sample. It can then be selected (cf. Fig. 5) how many randomly picked analyses out of these 25 will be used to calculate the $Fe^{3+}/\Sigma Fe$ of each sample. Figure 6 displays the result of such a calculation using an existing measurement series of 63 samples that has been measured with 25 analyses per sample. The shaded areas represent the 0.02 uncertainty of the method. As can be seen, 9-16 analyses per sample are already sufficient to obtain the same result as with 25 analyses per sample. Such an insight can significantly reduce the measurement time, *i.e.*, significantly increase the number of analyses per time. This tool therefore helps identify an optimum relationship between measurement time and number of analyses per sample. Flank Reduction allows to produce a plot such as Figure 6 within minutes from the dataset of a single measurement campaign.

In cases, some analyses obtained from a sample are poor, *e.g.*, have largely deviating element concentrations or totals that are either too low or too high.. This might happen when a sample is small, poorly polished or carbon-coated, heterogeneous or zoned on a small scale, or if the grain size is too small for a grid of points and requires placing the individual analyses points manually on different grains. The inspection tool allows identifying poor analyses by displaying all analyses of each sample in individual plots either for one element (Fig. 7) or plots of all elements from an individual sample. A colour coded box for each sample with the average value and its standard deviation provides quick information whether a sample might contain poor analyses. Each identified poor analysis can be indicated as such in the ’Inspected‘ column of a measurement spreadsheet. Simply adding an *e.g.*, ’x‘ before the sample name will essentially make this a new sample for the program. If the sample name is alternatively replaced by ‘ignore’, the entire analysis will be ignored. After all poor analyses have been identified and marked in the ’Inspected‘ column of the measurement spreadsheet, this needs to be uploaded again. It is then possible to select the ‘Inspected’ column as the sample name column. If names

in the 'Inspected' column were marked with *e.g.*, an 'x', and say three analyses were marked like this, then these three will be treated as a separate sample, *i.e.*, an $Fe^{3+}/\Sigma Fe$ will be calculated for this, and it will be displayed in its own plot. This has the advantage that the $Fe^{3+}/\Sigma Fe$ of the poor analyses can directly be compared to the analyses of the remaining good analyses. This might be informative to better understand the sample, *e.g.*, if individual spots were placed across a zonation, crack, or else. If an analysis name was replaced by 'ignore', it will not show up in the results or in a plot.

Each sample is bracketed by drift monitor measurements (*e.g.*, 5) to detect a possible change in $L\beta/L\alpha$, *e.g.*, due to temperature variations in the lab or a spectrometer drift during long measurement campaigns. An ideal drift monitor standard is high in Fe^{2+} (*e.g.*, almandine), which corresponds to a high $L\beta/L\alpha$. The stability of the $L\beta/L\alpha$ over the measurement campaign, as well as any other element or measured value can be inspected in 'Results Inspection' and 'Drift Monitor'. Unstable values of $L\beta/L\alpha$ directly translate into a variation in $Fe^{3+}/\Sigma Fe$. The drift monitor analyses might be used to correct the sample measurements accordingly.

4. Discussion

Flank Reduction allows for a fast, simple and GUI driven data reduction to determine $Fe^{3+}/\Sigma Fe$ in minerals such as garnet using microprobe data, and in addition provides valuable and relevant new insights. The Fe^{3+} Results Plot allows for a quick test which flank method standards are the most suitable for the studied samples. For example, if five standards were measured, four can be used to calculate the regression parameters, while the fifth is treated as unknown. After each of the five standards was treated as an unknown, the deviation of their determined $Fe^{3+}/\Sigma Fe$ from their real values provide clues towards which standard might skew

the results towards incorrect values. Further, systematic shifts on the dispersion of the lines of equal $Fe^{3+}/\Sigma Fe$ (cf. Fig. 2) can be identified when standards and/or samples with largely different $Fe^{3+}/\Sigma Fe$ are studied. The Fe^{3+} Results Plot then helps to determine how to possibly split such measurements into sub-campaigns, each of which measuring only standard-sample combinations that have similar ΣFe and $Fe^{3+}/\Sigma Fe$. Finally, the Fe^{3+} Results Plot illustrates the increasing precision of $Fe^{3+}/\Sigma Fe$ with increasing ΣFe, as the dispersion of the lines of equal $Fe^{3+}/\Sigma Fe$ increase with increasing ΣFe.

The precisions of the determined $Fe^{3+}/\Sigma Fe$ depend on the number of analyses per sample. Flank Reduction allows to find the minimum required number of analyses per sample without compromising on analytical precision (cf. Fig. 6). Choosing the right number of analyses per sample can reduce the measurement time significantly, thereby allowing to either save time and cost, or measure additional or repeated points, which will increase the reliability of the results.

The wide range of optional sample as well as result visualisations provide insights to analysis variations or trends by correlating elements, Lβ/Lα, probe current, $Fe^{3+}/\Sigma Fe$, and more. These tools are informative to identify and exclude outliers, instantly test the influence of such exclusions in re-runs, or understand the homogeneity of the studied samples. This straight-forward workflow of selecting the best analyses should allow for more robust results.

An exciting option of Flank Reduction is its expandability to determine the $Fe^{3+}/\Sigma Fe$ in additional minerals *e.g.*, pyroxene or amphibole. This is straight-forward, but requires a set of well-defined flank method standards with known values of $Fe^{3+}/\Sigma Fe$. These are then used in the same manner as *e.g.*, garnet standards. All tools of Flank Reduction can be used to test the validity of the standards in the same way as described above. Hence, Flank Reduction is not a dedicated app to determine $Fe^{3+}/\Sigma Fe$ in garnets, but universally applicable to other minerals after the flank method itself has been proven to be applicable to these minerals.

Finally, other visualisations, new functionalities, or simply suggestions for an enhanced workflow can be added to Flank Reduction. In fact, the program is constantly being developed and tweaked.

5. Implications

Studying the $Fe^{3+}/\Sigma Fe$ in minerals such as garnets provide important information about the formation of these minerals and their host rocks. Determining their $Fe^{3+}/\Sigma Fe$, however, was so far often hampered by either the availability of a suitable technique (Mössbauer, XANES) or required a complex data reduction process when using the EPMA flank method. The implementation of Flank Reduction as an open online tool written in a widespread open coding language makes the so far challenging to use data reduction process that was based on a proprietary program, intuitive, quick, simple, understandable, and easily expandable. This emphasises the potential and importance of research software, as well as the need for open and FAIR4RS publication. Clearly defining file formats and thereby following international conventions allows for synergies across software, for example, the measurement template as well as required Flank Reduction spreadsheet structure will both soon become part of ProbeSoftware[1].

The comprehensive documentation is embedded in a platform for modular or even distributed software. Additional research software is easily added, without requirements for specific formats. The documentation of such research software could be readily added to the platform as markdown files.

[1]https://probesoftware.com

Acknowledgements

We are grateful to two anonymous reviewers for their support in making this a better publication. We similarly thank the AE to improve this paper with his thoroughly review.

References

Barker M., Hong N. P. C., Katz D. S., Lamprecht A.-L., Martinez-Ortiz C., Psomopoulos F., Harrow J., Castro L. J., Gruenpeter M., Martinez P. A. and Honeyman T. (2022) Introducing the FAIR Principles for research software. Scientific Data 9, 622.

Enders, M., Speer, D., Maresch, W.V., and McCammon, C.A. (2000) Ferric/ferrous iron ratios in sodic amphiboles: Mössbauer analysis, stoichiometry-based model calculations and the high-resolution microanalytical flank method. Contributions to Mineralogy and Petrology, 140, 135-147.

Gudelius D, Aulbach S, Braga R, Höfer H, Woodland AB, Gerdes A (2019): Element transfer and redox conditions in continental subduction zones: New insights from peridotites of the Ulten Zone (N Italy). Journal of Petrology 60: 231-268

Höfer H. E. (2002) Quantification of Fe^{2+}/Fe^{3+} by Electron Microprobe Analysis – New Developments. Hyperfine Interactions 144–145, 239–248.

Höfer H. E. and Brey G. P. (2007) The iron oxidation state of garnet by electron microprobe: Its determination with the flank method combined with major-element analysis. American Mineralogist 92, 873–885.

Höfer, H. E., Brey, G. P., Schulz-Dobrick, B., and Oberhänsli, R. (1994) The determination of the oxidation state of iron by the electron microprobe. European Journal of Mineralogy, 6, 407-418.

Höfer, H. E., Brey, G. P., and Oberhänsli, R. (1996) The determination of the oxidation state of iron in synthetic garnets by X-ray spectroscopy with the electron microprobe. Physics and Chemistry of Minerals, 23, 241.

Höfer H. E., Weinbruch S., McCammon C. A. and Brey G. P. (2000) Comparison of two electron probe microanalysis techniques to determine ferric iron in synthetic wüstite samples. European Journal of Mineralogy 12, 63–71.

Höfer H. E., Brey, G. P., and Hibberson, W. O. (2004) Iron oxidation state determination in synthetic pyroxenes by electron microprobe. Lithos, 73, 551.

Höfer, H.E., Brey, G.P., Shu, Q., Heckel, C., & Vasilyev, P. (2017). Redox state of Archean kyanite/corundum eclogites and garnet pyroxenites from Bellsbank, South Africa. International Kimberlite Conference: Extended Abstracts, 11.

Klöcking M, Wyborn L, Lehnert KA, Ware B, Prent AM, Profeta L, Kohlmann F, Noble W, Bruno I, Lambart S, Ananuer H, Barber ND, Becker H, Brodbeck M, Deng H, Deng K, Elger K, Franco GdS, Gao Y, Ghasera KM, Hezel DC, Huang J, Kerswell B, Koch H, Lanati AW, Maat Gt, Martínez-Villegas N, Yobo LN, Redaa A, Schäfer W, Swing MR, Taylor RJM, Traun MK, Whelan J, Zhou T (2023) Community recommendations for geochemical data, services and analytical capabilities in the 21st century. Geochimica et Cosmochimica Acta (in press) [doi: 10.1016/j.gca.2023.04.024]

Lehnert, K., Wyborn, L., Bennett, V.C., Hezel, D.C., McInnes, B.I.A., Plank, T., Rubin, K., 2021. Onegeochemistry: Towards an interoperable global network of fair geochemical data URL: https://zenodo.org/record/5767950

Longo, M., McCammon, C.A., Jacobsen, S.D. (2011): Microanalysis of the iron oxidation state in (Mg,Fe)O and application to the study of microscale processes. Contributions to Mineralogy and Petrology, 162, 1249-1257.

Malaspina, N., Poli, S., Fumagalli, P. (2009): The Oxidation State of Metasomatized Mantle Wedge: Insights from C-O-H-bearing Garnet Peridotite. Journal of Petrology 50, 1533-1552.

Malaspina, N., Scambelluri, M., Poli, S., Van Roermund, H.L.M., Langenhorst, F. (2010): The oxidation state of mantle wedge majoritic garnet websterites metasomatised by C-bearing subduction fluids. Earth and Planetary Science Letters 298, 417-426.

McCammon, C.A., Chaskar, V., and Richards, G.G. (1991) A technique for spatially resolved Mössbauer spectroscopy applied to quenched metallurgical slags. Measurement Science and Technology, 2, 657-662.

Tang M, Lee C-TA, Costin G, Höfer HE (2019): Recycling reduced iron at the base of magmatic orogens. Earth and Planetary Science Letters 528, 115827.

Tao R., Fei Y., Bullock E.S., Xu C., Zhang L., (2018): Experimental investigation of Fe^{3+}-rich majoritic garnet and its effect on majorite geobarometer. Geochimica et Cosmochimica Acta 225, 1-16

Tao R., Zhang L., Tian M., Zhu J., Liu X., Liu J., Höfer H.E., Stagno V., Fei Y. (2018): Formation of abiotic hydrocarbon from reduction of carbonate in subduction zones: Constraints from petrological observation and experimental simulation. Geochimica et Cosmochimica Acta 239, 390-408

Wang C, Tao R, Walters JB, Höfer HE, Zhang L (2022): Favorable P–T–*f*O2 conditions for abiotic CH4 production in subducted oceanic crusts: A comparison between CH4-bearing ultrahigh- and CO2-bearing high-pressure eclogite. Geochimica et Cosmochimica Acta 336, 269-290.

Wilkinson, M.D., Dumontier, M., Aalbersberg, I.J., Appleton, G., Axton, M., Baak, A., Blomberg, N., Boiten, J.W., da Silva Santos, L.B., Bourne, P.E., Bouwman, J., Brookes, A.J., Clark, T., Crosas, M., Dillo, I., Dumon, O., Edmunds, S., Evelo, C.T., Finkers, R., Gonzalez-Beltran, A., Gray, A.J., Groth, P., Goble, C., Grethe, J.S., Heringa, J., 't Hoen, P.A., Hooft, R., Kuhn, T., Kok, R., Kok, J., Lusher, S.J., Martone, M.E., Mons, A., Packer, A.L., Persson, B., Rocca-Serra, P., Roos, M., van Schaik, R., Sansone, S.A., Schultes, E., Sengstag, T., Slater, T., Strawn, G., Swertz, M.A., Thompson, M., van der Lei, J., van Mulligen, E., Velterop, J., Waagmeester, A., Wittenburg, P., Wolstencroft, K., Zhao, J., Mons, B., 2016. The FAIR guiding principles for scientific data management and stewardship. Scientific Data 3.

Zhang C., Almeev R.R., Hughes E.C., Borisov A. A., Wolff E.P., Höfer H.E., Botcharnikov R. and Koepke J (2018): Electron microprobe technique for the determination of iron oxidation state in silicate glasses. American Mineralogist 103, 1445-1454.

Figure captions

Fig. 1: EPMA FeLα and FeLβ-spectra from an almandine (Fe^{3+}-poor) and an andradite (Fe^{3+}-rich). For the orange line –the 'difference spectrum' –, the almandine spectrum was subtracted from the andradite spectrum. The vertical, dashed lines indicate optimal analyser crystal positions at the minima/maxima of the difference spectrum.

Fig. 2: a) Fe^{3+} Results Plot calculated from 4 flank method standards (large symbols) and with an example set of 63 samples. Lines represent equal $Fe^{3+}/\Sigma Fe$. Lβ/Lα ratios were obtained redundantly from two spectrometers, hence, the plots contain a regression for each spectrometer (blue and orange, respectively). b) Same as a), but the regressions were calculated from 5 flank method standards, including one andradite.

Fig. 3: Schematic flow chart for the flank method workflow. Steps 1 & 4 are completely redesigned and the core of this paper. In particular, the data reduction step 4 is now an open, online tool and allows the fast, GUI driven calculation of $Fe^{3+}/\Sigma Fe$.

Fig. 4: The same as Figure 1, but demonstrating that small interval spectra are fully sufficient to determine the optimum analyser crystal positions.

Fig. 5: The GUI to upload data and control how the $Fe^{3+}/\Sigma Fe$ calculation is performed.

Fig. 6: The $Fe^{3+}/\Sigma Fe$ of each sample is calculated from the average of 25 analyses. From these 25 analyses, smaller numbers have been randomly chosen – these are indicated in the legend –, and from these the $Fe^{3+}/\Sigma Fe$ of each sample was recalculated. The shadowed area represents a constant 0.02 error, which is a typical error of this method. a) and b) are the same plots, with b) showing lesser calculated results.

Fig. 7: The quality of all analyses on each sample can be inspected on individual plots with colour coded indications for the magnitude of the standard deviation. The x-axis are the point numbers.

This is the peer-reviewed, final accepted version for American Mineralogist, published by the Mineralogical Society of America.
The published version is subject to change. Cite as Authors (Year) Title. American Mineralogist, in press.
DOI: https://doi.org/10.2138/am-2023-9112. http://www.minsocam.org/

Figures

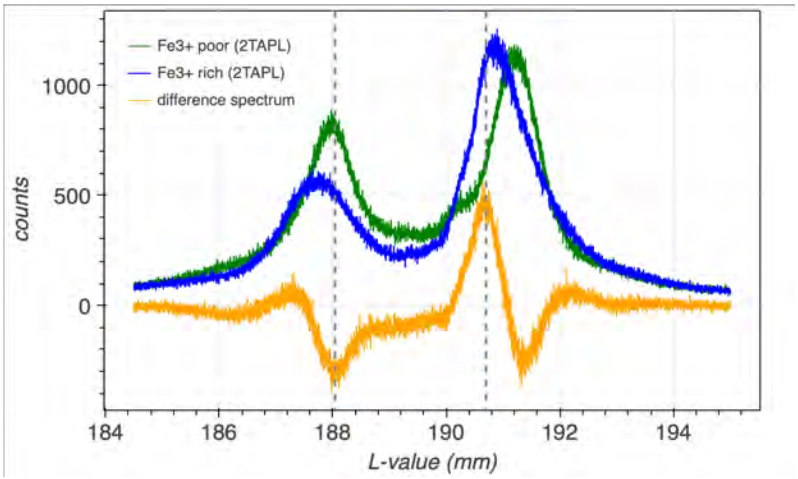

Fig. 1

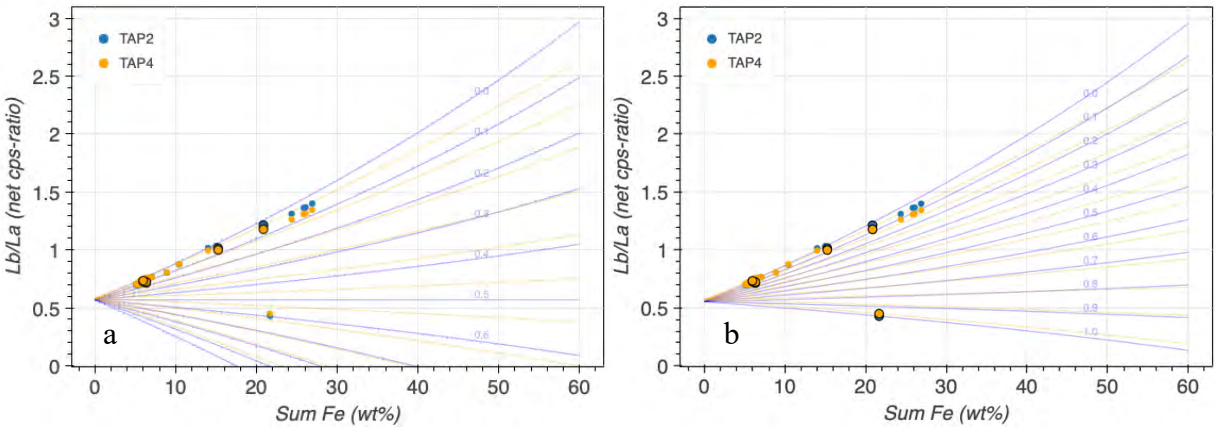

Fig. 2

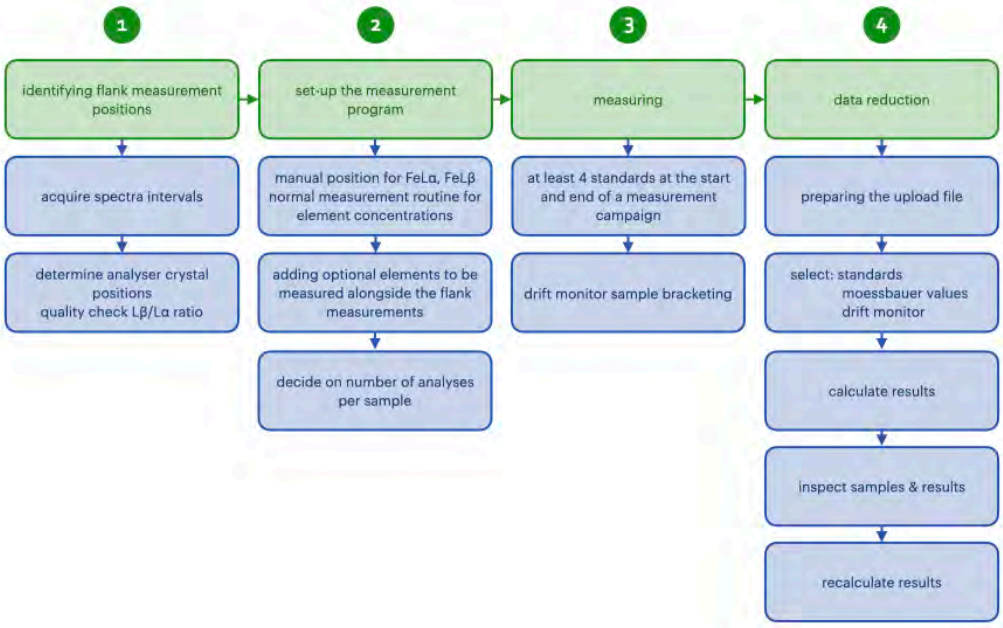

Fig. 3

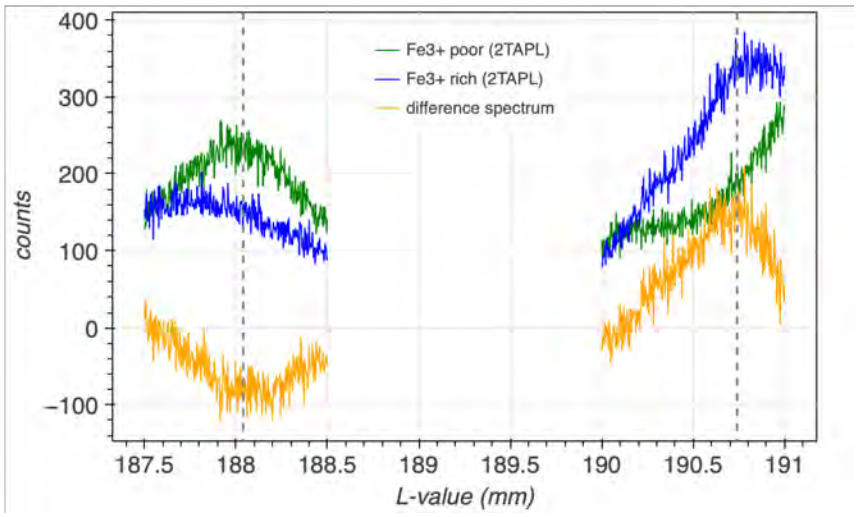

Fig. 4

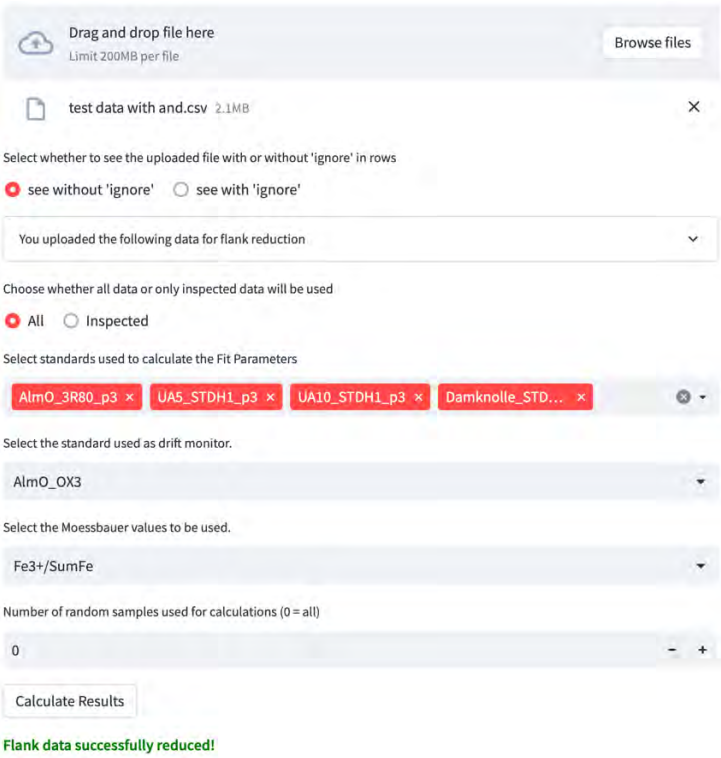

Fig. 5

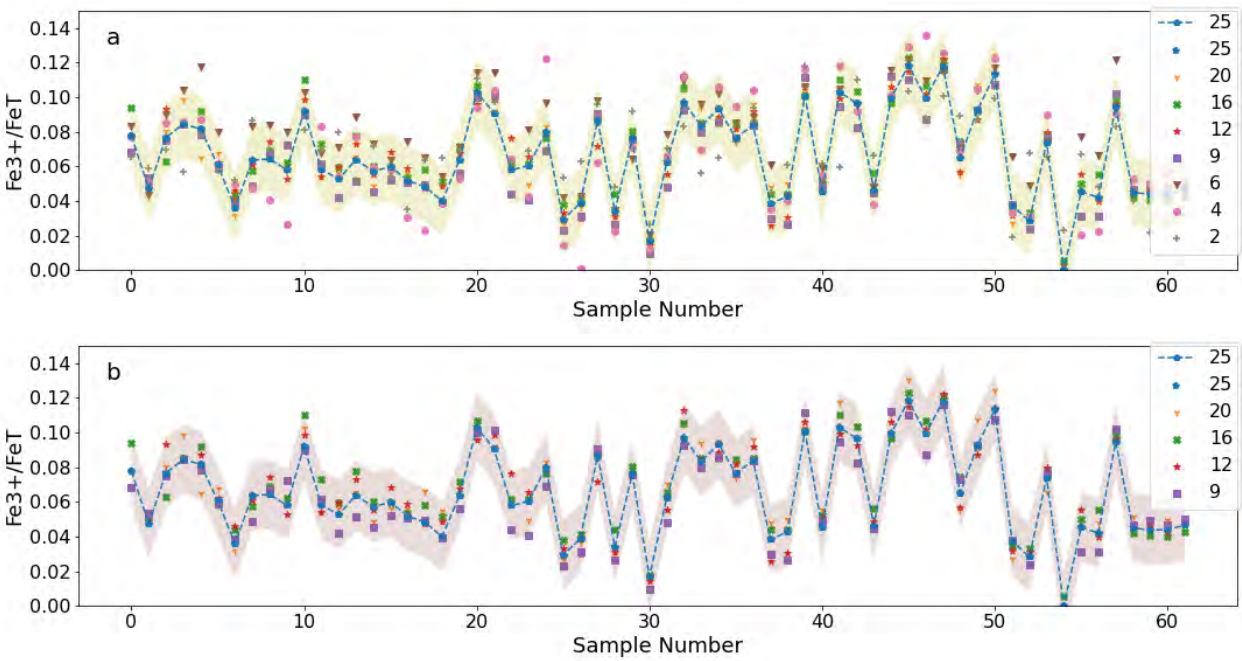

Fig. 6

This is the peer-reviewed, final accepted version for American Mineralogist, published by the Mineralogical Society of America.
The published version is subject to change. Cite as Authors (Year) Title. American Mineralogist, in press.
DOI: https://doi.org/10.2138/am-2023-9112. http://www.minsocam.org/

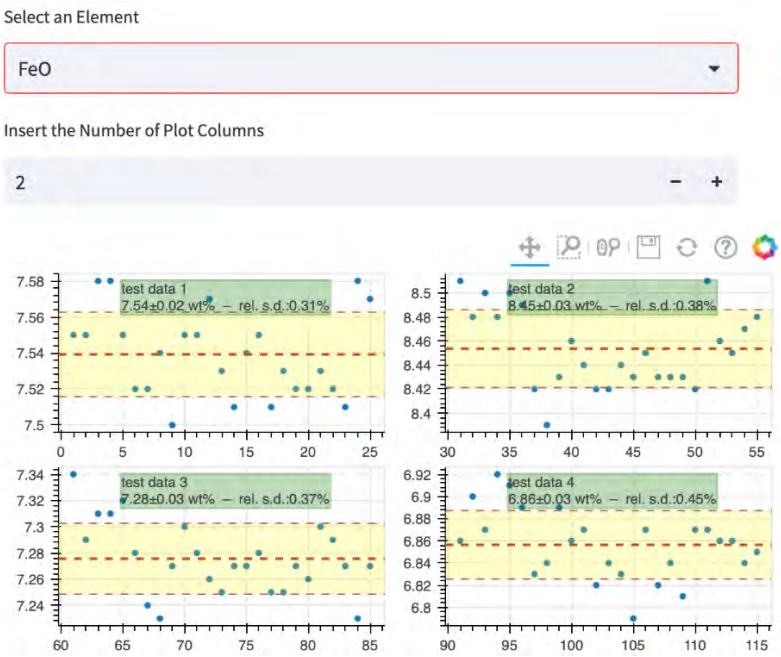

Fig. 7